

# Traveling wave parametric amplifier with Josephson junctions using minimal resonator phase matching

T. C. White,<sup>1,a)</sup> J. Y. Mutus,<sup>1,a),b)</sup> I.-C. Hoi,<sup>1</sup> R. Barends,<sup>1,b)</sup> B. Campbell,<sup>1</sup> Yu Chen,<sup>1,b)</sup> Z. Chen,<sup>1</sup> B. Chiaro,<sup>1</sup> A. Dunsworth,<sup>1</sup> E. Jeffrey,<sup>1,b)</sup> J. Kelly,<sup>1</sup> A. Megrant,<sup>1,2</sup> C. Neill,<sup>1</sup> P. J. J. O'Malley,<sup>1</sup> P. Roushan,<sup>1,b)</sup> D. Sank,<sup>1,b)</sup> A. Vainsencher,<sup>1</sup> J. Wenner,<sup>1</sup> S. Chaudhuri,<sup>3</sup> J. Gao,<sup>4</sup> and John M. Martinis<sup>1,b),c)</sup>

<sup>1</sup>Department of Physics, University of California, Santa Barbara, California 93106-9530, USA

<sup>2</sup>Department of Materials, University of California, Santa Barbara, California 93106, USA

<sup>3</sup>Department of Physics, Stanford University, Stanford, California 94305, USA

<sup>4</sup>National Institute of Standards and Technology, Boulder, Colorado 80305, USA

(Received 14 March 2015; accepted 30 April 2015; published online 15 June 2015)

Josephson parametric amplifiers have become a critical tool in superconducting device physics due to their high gain and quantum-limited noise. Traveling wave parametric amplifiers (TWPAs) promise similar noise performance, while allowing for significant increases in both bandwidth and dynamic range. We present a TWPA device based on an LC-ladder transmission line of Josephson junctions and parallel plate capacitors using low-loss amorphous silicon dielectric. Crucially, we have inserted  $\lambda/4$  resonators at regular intervals along the transmission line in order to maintain the phase matching condition between pump, signal, and idler and increase gain. We achieve an average gain of 12 dB across a 4 GHz span, along with an average saturation power of  $-92$  dBm with noise approaching the quantum limit. © 2015 AIP Publishing LLC.

[<http://dx.doi.org/10.1063/1.4922348>]

The Josephson parametric amplifier<sup>1–7</sup> (JPA) is a critical tool for high fidelity state measurement in superconducting qubits<sup>8–10</sup> as it allows parametric amplification with near quantum-limited noise.<sup>11</sup> Despite its success, the JPA has typically been used only for single frequency measurements due to lower bandwidth and saturation power. A promising approach to scaling superconducting qubit experiments is frequency multiplexing,<sup>12–14</sup> which requires additional bandwidth and dynamic range for each measurement tone. Simultaneous amplification of up to five multiplexed tones has been achieved with a JPA<sup>15–17</sup> but was only possible with the Impedance-transformed parametric amplifier<sup>18</sup> (IMPA). This highly engineered JPA provides much larger bandwidth and saturation power but pushes the resonant design to its low  $Q$  limit.

To extend this frequency multiplexed approach for future experiments, we have adopted the distributed design of the traveling wave parametric amplifier (TWPA).<sup>19</sup> Fiber-optic TWPAs have already demonstrated high gain, dynamic range, and bandwidth while reaching the quantum-limit of added noise.<sup>20,21</sup> In this letter, we present a microwave frequency TWPA with 4 GHz of bandwidth and an order of magnitude more saturation power than the best JPA. This device is compatible with scaling to much larger qubit systems through multiplexed measurement, and may find applications outside quantum information such as astrophysics detectors.<sup>12,22</sup>

At microwave frequencies, the TWPA can be thought of as a transmission line, where the propagation velocity is controlled by varying the individual circuit parameters of

inductance or capacitance per unit length.<sup>24,25</sup> This is typically achieved by constructing a signal line with a current dependent (nonlinear) inductance. Like the JPA, a large enough pump tone will modulate this inductance, coupling the pump ( $\omega_p$ ) to a signal ( $\omega_s$ ) and idler ( $\omega_i$ ) tone via frequency mixing such that  $\omega_s + \omega_i = 2\omega_p$ . Unlike the JPA, however, the TWPA has no resonant structure so gain, bandwidth, and dynamic range are determined by the coupled mode equations of a nonlinear transmission line.<sup>23</sup> In addition to allowing more bandwidth and saturation power, the TWPA is directional so that amplification only occurs for signals propagating in the same direction as the pump.

The concept of a nonlinear superconducting transmission line has been demonstrated in NbTiN TWPA,<sup>26</sup> where the kinetic inductance of the superconductor provides nonlinearity in a standard co-planar waveguide (CPW). These amplifiers have achieved gains greater than 20 dB over bandwidths greater than 8 GHz, and with saturation power many orders of magnitude larger than a standard JPA. To achieve this high dynamic range, a large pump tone ( $\sim 100 \mu\text{W}$ ) is required, which poses many engineering challenges for qubit readout. Attenuation in the line leads to heating which increases the base temperature of the experiment. Likely due to this local heating, the NbTiN amplifier has yet to reach the quantum limit of added noise. In addition, the qubits must be aggressively isolated from the large pump tone which requires additional hardware.

The ideal amplifier for qubit readout would provide gain and bandwidth similar to the NbTiN TWPA but with a higher non-linearity, requiring less pump power and achieving quantum-limited noise. A promising approach is to build a TWPA based on the non-linear inductance of the Josephson junction (JJ).<sup>27–30</sup> This junction TWPA (JTWPA) circuit, shown in Fig. 1(a), combines JJs with shunt

<sup>a)</sup>T. C. White and J. Y. Mutus contributed equally to this work.

<sup>b)</sup>Present address: Google, Santa Barbara, California 93117, USA.

<sup>c)</sup>martinis@physics.ucsb.edu

capacitors to construct a 50  $\Omega$  lumped element transmission line. The capacitors and JJs are small relative to the wavelength of a microwave signal, giving an effective capacitance and non-linear inductance per unit length. The JTWPA obeys the same physics as the NbTiN TWPA, but needs  $\sim 10^5$  times less pump power.

TWPA gain is described by solving the coupled mode equations including mixing terms between the pump ( $k_p$ ), signal ( $k_s$ ), and idler ( $k_i$ ) wave vectors.<sup>23</sup> Power gain is given by

$$G_s = \cosh^2(gz) + \left(\frac{\kappa}{2g}\right)^2 \sinh^2(gz) \quad (1)$$

and

$$g = \sqrt{\frac{k_s k_i}{k_p^2} (\gamma k_p)^2 - (\kappa/2)^2}. \quad (2)$$

Here,  $z$  is the length along the transmission line,  $\gamma = I_p^2/16I_c^2$  describes the ratio of drive current to junction critical current (nonlinearity), and  $\kappa = 2\gamma k_p + k_s + k_i - 2k_p$  is the effective dispersion. The pre-factor  $k_s k_i/k_p^2$  describes the bandwidth of the amplifier and maximizes gain when  $k_s = k_i = k_p$ . For small signal powers where  $\gamma \approx 0$ ,  $\kappa$  would be described by the difference in wave vectors  $\Delta k = k_s + k_i - 2k_p$ . The term  $2\gamma k_p$  describes the self phase modulation of the pump, shown

in Fig. 1(b), which increases with pump power. In a linear superconducting transmission line there is no dispersion, so  $\Delta k \approx 0$  making  $\kappa \approx 2\gamma k_p$ . The maximum gain then occurs when  $g \approx 0$  and is given by

$$G_s = 1 + (\gamma k_p z)^2 = 1 + \phi_{nl}^2, \quad (3)$$

where  $\phi_{nl} = \gamma k_p z$  is the nonlinear phase shift of the pump such that gain depends quadratically on length. If proper phase matching can be achieved,  $\kappa = 0$ ,  $g = \gamma k_p$ , and the maximum gain, given by

$$G_s = \cosh^2(\gamma k_p z) \approx \frac{\exp(2\phi_{nl})}{4}, \quad (4)$$

is exponentially dependent on length. The phase matched design thus provides a much larger gain-bandwidth than a non phase matched TWPA for a given number of junctions and is a more efficient amplifier design.

To produce  $\kappa = 0$ , we can counter the power-dependent phase shift of the pump with an engineered frequency-tunable phase shift. In the NbTiN TWPAs, this was accomplished by a periodic impedance variation which created a narrow band gap and phase shift in the transmission.<sup>31</sup> However, this approach provides only a small correction to the phase shift per unit length, which is incompatible with the high nonlinear phase shifts of the JTWPA. Alternatively, a resonator capacitively coupled to the transmission line, shown in Fig. 1(c), produces an arbitrarily large frequency dependent phase shift which counters the non-linear phase shift. By including such a resonator after every nonlinear section in the transmission line, shown in Fig. 1(d), the pump frequency could be tuned to cancel the phase mismatch; thus making  $\kappa \approx 0$ . This approach has been shown to significantly increase both gain and bandwidth for a given number of junctions.<sup>30,32</sup>

While continuous phase correction is the most obvious approach, a resonator following each junction can introduce additional complications. The large number of resonators would require a compact lumped-element design with parallel plate capacitors. The frequency of these resonators would be harder to control and the extra dielectric will introduce more loss. It should be possible however, to use fewer total resonators if we increase the phase shift from each individual resonator. With fewer total resonators we can use larger CPW designs with lower loss and greater frequency control. The concept of discrete phase correction is shown in Fig. 1(e).

Our device, shown in Fig. 2(a), consists of a single 66 mm CPW with both non-linear (lumped element JJ array) and linear (superconducting Al) sections. The 1326 JJs are standard Al-Al<sub>2</sub>O<sub>3</sub>-Al junctions created using double angle evaporation.<sup>33</sup> The junction critical current was designed to be 5  $\mu$ A with an effective inductance of 65 pH per junction that, combined with geometric inductance, gives 3.5  $\mu$ H/m. Parallel plate capacitors made with low loss amorphous silicon (a-Si:H) dielectric<sup>34</sup> provide 1.6 nF/m in the non-linear sections of the chip, setting the impedance while also shorting together the ground planes. Connecting the ground planes is important because such a long transmission line

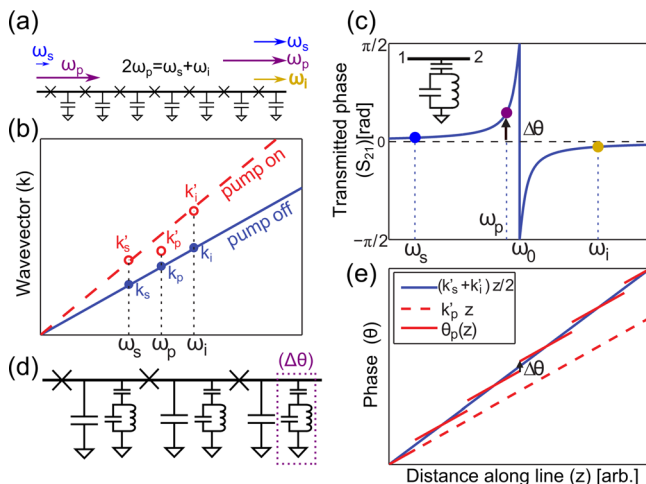


FIG. 1. (a) Circuit diagram of the Josephson junction TWPA. (b) The dispersion relationship in a conventional Josephson junction TWPA. For weak signals (linear regime), the dispersion is linear  $\Delta k = k_s + k_i - 2k_p = 0$ , where  $k = \omega/v_p$ . When a strong pump tone is applied, the traveling waves are slowed down due to an increase in the junction inductance and a decrease in the phase velocity. The pump tone is slowed down less than the signal and idler tones due to the difference between the self-phase modulation and cross-phase modulation<sup>23</sup> effects which causes a mismatch  $\Delta k' > 0$ . (c) Phase shift due to a shunt resonator to ground. The resonator produces a frequency dependent phase shift for just the pump tone. (d) Resonantly phase matched TWPA, in which resonator phase shifters are inserted between nonlinear transmission line sections. (e) The phase of the pump tone is adjusted at discrete locations and piece-wise matched to the signal and idler tones which enhances the gain, as can be seen from a tight fit between the stepped solid red line and the straight blue line  $\Delta k = 0$ . Without these resonator phase shifters, the phase mismatch would grow (as can be seen from the departure of the dashed red line from the solid blue line) and the gain would be limited to the quadratic case of Eq. (3).

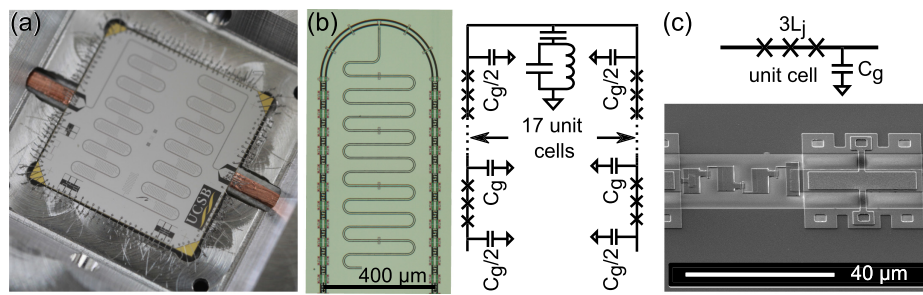


FIG. 2. (a) Photograph of the TWPA showing the full packaged device with an aluminum box and copper circuit-board feed lines. The chip is square with 6 mm sides. (b) Optical micrograph and circuit diagram that show the discrete phase matching through the periodic insertion of  $\lambda/4$  CPW resonators, spaced at an electrical length equivalent to  $\lambda/2$  of the pump tone. (c) Scanning electron micrograph of the non-linear unit cell consisting of three double angle evaporation Josephson junctions (left) and a shunt parallel plate capacitor (right), with amorphous silicon dielectric.

could support lossy slot line modes. The periodic structure shown in Fig. 2(b) consists of a series of JJs followed by a linear section where the resonator is used to fix the pump phase before entering the next non-linear section. To improve the impedance matching of the non-linear sections, the first and last shunt capacitor is half the capacitance of the others. We chose a nonlinear unit cell of three junctions per capacitor, shown in Fig. 2(c), to lower the transmission line cutoff frequency while maintaining a high junction critical current. This was done to prevent leakage of pump power into higher harmonics, which may reduce gain, and to prevent the onset of a shock wave.<sup>35</sup>

In the case of 1000 junctions, continuous phase matching can be approximated with the phase shift of just 10 ideal phase shifters.<sup>23</sup> This result however does not consider the effect of the resonant amplitude dip on the pump, which can lead to large reflected pump energy. Using more resonators will lessen this effect, but increase design complexity. However, if the  $\lambda/4$  resonators are spaced by  $(2n)\lambda/4$ , where  $\lambda$  is the wavelength corresponding to the resonator frequency, the periodic placement provides a large stop band at  $3\omega$  to prevent pump leakage. To take advantage of this enhancement on a chip with 1326 junctions, we chose 26 resonators with 17 non-linear unit cells between each resonator.

The resonance coming from the periodic placement combines with the resonators to create a sharp amplitude dip at 6.1 GHz with optimal phase shift at about 5.8 GHz, where almost no pump energy is reflected.

In the past, JTWPAs have had difficulty reaching the quantum limit of added noise due to loss in the transmission line.<sup>29</sup> To characterize the loss and transmission line performance in our device, we measured the amplitude of  $S_{21}$  and  $S_{11}$  through both the TWPA and a copper cable of equivalent length. We used *in-situ* microwave switches to alternate between the cable and the TWPA in the same experimental setup.<sup>23</sup> We find that the difference in  $S_{21}$  is less than 0.5 dB over the entire 4–8 GHz measurement band. When measuring  $S_{11}$  of the TWPA we see an average reflected amplitude  $-10$  dB relative to the cable  $S_{21}$ . This is consistent with the majority of the signal difference between the TWPA and the cable coming from reflections due to imperfect impedance matching.<sup>23</sup>

The device presented in Fig. 2(a) provides a good test of amplifier performance, but is limited to 6–8 dB gain. To increase the gain and verify the phase matching will hold in a longer device we chain two of these chips together in series. The performance of this amplifier chain is shown in Fig. 3 and it details the 1 dB compression point (saturation

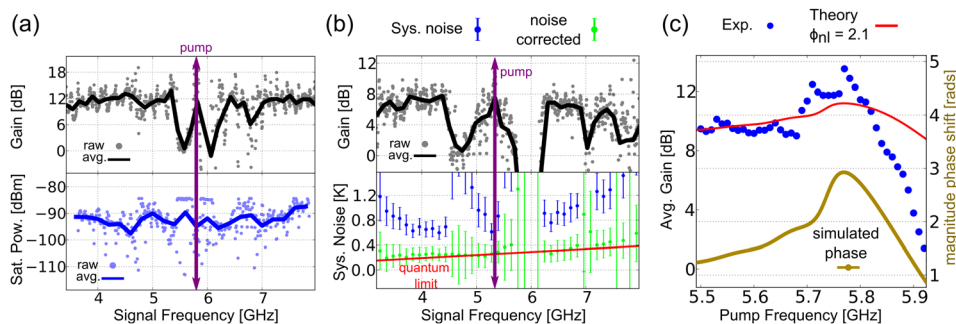


FIG. 3. (a) Saturation power and gain vs frequency for optimal pump gain with two TWPAs chained together; the pump tone is 5.83 GHz. Raw data are plotted in lighter points with a darker averaged line overlaying the data. Average saturation power is  $-92$  dBm and average gain is 12–14 dB. The dips on either side of the pump come from the resonator reflecting either the signal or the idler tone close to the pump. (b) Gain and system noise vs frequency for a subsequent experiment optimized for low noise at a pump tone of 5.32 GHz. In this subsequent experiment using the two chained devices from (a), the maximum gain achieved was only 8 dB, while the lowest noise was 600 mK corresponding to an input noise of two photons. The raw system noise is plotted in blue (dark), while system noise with the contribution from the HEMT subtracted is plotted in green (light). (c) Average gain and simulated phase shift vs frequency measured for a pair of devices which achieved 12–14 dB max gain. The blue (dark) data points are the averaged gain values, the yellow (light) curve is the simulated resonator phase shift after including realistic experimental conditions, and the red (solid dark) line is a theoretical gain curve computed using the simulated phase shift. The change from linear to exponential is consistent with  $\phi_{nl} \approx 2.1$  with a peak at 5.8 GHz.

power), gain, and noise temperature. Each chip was in a separate box and the boxes were connected via SMA connectors. The gain was measured relative to the low power transmission amplitude.

As can be seen in Fig. 3(a), the chained device displays an average gain of 12–14 dB over almost the entire 4–8 GHz frequency range. Interestingly, the gain dips quite significantly on either side of the pump. This is due to the reflection of either the signal or idler tone when measuring close to the pump frequency. Variations in the gain on the order of 2–3 dB most likely come from imperfect impedance matching between sections and at the bond pads. These variations in gain also affect the saturation power, here defined as the 1 dB compression point. The broad band input saturation power shown in Fig. 3(a) varies from –95 dBm to –85 dBm with an average of –92 dBm. This represents a significant improvement in both bandwidth and saturation power over the best resonant JPA.<sup>18</sup> The reverse gain measured was 0 dB as expected from the directionality of the coupled mode equations.<sup>23</sup>

To measure noise temperature, we used the method of signal to noise ratio improvement<sup>4,23</sup> over a traditional high electron mobility (HEMT) semiconductor amplifier.<sup>36</sup> In this experiment, the HEMT noise temperature was measured to be  $2.5 \pm 0.5$  K over the measurement band. The noise temperature measurement was conducted in a subsequent experiment using the two chained devices. Unfortunately due to sample aging, the largest gain achieved in this experiment, shown in Fig. 3(b), reached only 8 dB at a different pump power and frequency. In this case, we find that the noise does approach the quantum limit over the entire range but reaches a low of only 600 mK. This noise temperature corresponds to about two photons of input noise, and is consistent with residual HEMT noise at low gain. If we subtract the expected HEMT contribution to the system noise we find the noise added by the TWPA is very close to quantum limit.

To verify the frequency dependent phase correction, we measured average gain vs pump frequency for the chained device. The dependence of the gain on pump frequency is shown in Fig. 3(c) along with a simulated phase shift coming from the complete dispersion engineering. The shape of the phase shift is a result of the combined effects of both the individual resonators and the periodic spacing between them. The average gain increases by  $\sim 5$  dB when the pump nears the resonator phase shift. This is consistent with a nonlinear phase shift  $\phi_{nl} \approx 2.1$  with a predicted device gain plotted with a solid red line along with the data.

We have experimentally demonstrated a Josephson junction traveling wave parametric amplifier with minimal resonator phase matching. This amplifier displays a significant increase in both bandwidth and saturation power while maintaining near quantum-limited noise performance. By using discrete resonators to correct the pump phase, we can access the exponential gain dependence with a minimal increase in fab complexity. In this regime, we should be able to increase the gain by simply increasing the length of the device. In addition, it may be possible to improve the transmission amplitude even further through fine tuning of the impedance in each section.

This work was supported by the Office of the Director of National Intelligence (ODNI), Intelligence Advanced Research Projects Activity (IARPA), through the Army Research Office Grant W911NF-10-1-0334. All statements of fact, opinion, or conclusions contained herein are those of the authors and should not be construed as representing the official views or policies of IARPA, the ODNI, or the U.S. Government. Devices were made at the UC Santa Barbara Nanofabrication Facility, a part of the NSF-funded National Nanotechnology Infrastructure Network, and at the NanoStructures Cleanroom Facility.

- <sup>1</sup>B. Yurke, L. Corruccini, P. Kaminsky, L. Rupp, A. Smith, A. Silver, R. Simon, and E. Whittaker, *Phys. Rev. A* **39**, 2519 (1989).
- <sup>2</sup>T. Yamamoto, K. Inomata, M. Watanabe, K. Matsuba, T. Miyazaki, W. Oliver, Y. Nakamura, and J. Tsai, *Appl. Phys. Lett.* **93**, 042510 (2008).
- <sup>3</sup>M. Castellanos-Beltran and K. Lehnert, *Appl. Phys. Lett.* **91**, 083509 (2007).
- <sup>4</sup>M. Hatridge, R. Vijay, D. Slichter, J. Clarke, and I. Siddiqi, *Phys. Rev. B* **83**, 134501 (2011).
- <sup>5</sup>B. Abdo, F. Schackert, M. Hatridge, C. Rigetti, and M. Devoret, *Appl. Phys. Lett.* **99**, 162506 (2011).
- <sup>6</sup>J. Mutus, T. White, E. Jeffrey, D. Sank, R. Barends, J. Bochmann, Y. Chen, Z. Chen, B. Chiaro, A. Dunsworth *et al.*, *Appl. Phys. Lett.* **103**, 122602 (2013).
- <sup>7</sup>C. Eichler, Y. Salathe, J. Mlynek, S. Schmidt, and A. Wallraff, *Phys. Rev. Lett.* **113**, 110502 (2014).
- <sup>8</sup>R. Vijay, D. Slichter, and I. Siddiqi, *Phys. Rev. Lett.* **106**, 110502 (2011).
- <sup>9</sup>M. Hatridge, S. Shankar, M. Mirrahimi, F. Schackert, K. Geerlings, T. Brecht, K. Sliwa, B. Abdo, L. Frunzio, S. Girvin *et al.*, *Science* **339**, 178 (2013).
- <sup>10</sup>K. Murch, S. Weber, C. Macklin, and I. Siddiqi, *Nature* **502**, 211 (2013).
- <sup>11</sup>C. M. Caves, *Phys. Rev. D* **26**, 1817 (1982).
- <sup>12</sup>P. K. Day, H. G. LeDuc, B. A. Mazin, A. Vayonakis, and J. Zmuidzinas, *Nature* **425**, 817 (2003).
- <sup>13</sup>Y. Chen, D. Sank, P. O'Malley, T. White, R. Barends, B. Chiaro, J. Kelly, E. Lucero, M. Mariantoni, A. Megrant *et al.*, *Appl. Phys. Lett.* **101**, 182601 (2012).
- <sup>14</sup>O.-P. Saira, J. Groen, J. Cramer, M. Meretska, G. De Lange, and L. DiCarlo, *Phys. Rev. Lett.* **112**, 070502 (2014).
- <sup>15</sup>E. Jeffrey, D. Sank, J. Mutus, T. White, J. Kelly, R. Barends, Y. Chen, Z. Chen, B. Chiaro, A. Dunsworth *et al.*, *Phys. Rev. Lett.* **112**, 190504 (2014).
- <sup>16</sup>R. Barends, J. Kelly, A. Megrant, A. Veitia, D. Sank, E. Jeffrey, T. White, J. Mutus, A. Fowler, B. Campbell *et al.*, *Nature* **508**, 500 (2014).
- <sup>17</sup>J. Kelly, R. Barends, A. Fowler, A. Megrant, E. Jeffrey, T. White, D. Sank, J. Mutus, B. Campbell, Y. Chen *et al.*, *Nature* **519**, 66 (2015).
- <sup>18</sup>J. Mutus, T. White, R. Barends, Y. Chen, Z. Chen, B. Chiaro, A. Dunsworth, E. Jeffrey, and J. O. Kelly, *Appl. Phys. Lett.* **104**, 263513 (2014).
- <sup>19</sup>O. Yaakobi, L. Friedland, C. Macklin, and I. Siddiqi, *Phys. Rev. B* **87**, 144301 (2013).
- <sup>20</sup>J. Armstrong, N. Bloembergen, J. Ducuing, and P. Pershan, *Phys. Rev.* **127**, 1918 (1962).
- <sup>21</sup>P. Kumar, O. Aytür, and J. Huang, *Phys. Rev. Lett.* **64**, 1015 (1990).
- <sup>22</sup>S. J. Asztalos, G. Carosi, C. Haggmann, D. Kinion, K. Van Bibber, M. Hotz, L. Rosenberg, G. Rybka, J. Hoskins, J. Hwang *et al.*, *Phys. Rev. Lett.* **104**, 041301 (2010).
- <sup>23</sup>See supplementary material at <http://dx.doi.org/10.1063/1.4922348> for further description of sample, measurements, and equations.
- <sup>24</sup>A. Cullen, *Nature* **181**, 332 (1958).
- <sup>25</sup>P. Tien, *J. Appl. Phys.* **29**, 1347 (1958).
- <sup>26</sup>B. H. Eom, P. K. Day, H. G. LeDuc, and J. Zmuidzinas, *Nat. Phys.* **8**, 623–627 (2012).
- <sup>27</sup>S. Wahlsten, S. Rudner, and T. Claeson, *Appl. Phys. Lett.* **30**, 298 (1977).
- <sup>28</sup>M. Feldman, P. Parrish, and R. Chiao, *J. Appl. Phys.* **46**, 4031 (1975).
- <sup>29</sup>B. Yurke, M. Roukes, R. Movshovich, and A. Pargellis, *Appl. Phys. Lett.* **69**, 3078 (1996).
- <sup>30</sup>C. Macklin (unpublished).

- <sup>31</sup>C. Bockstiegel, J. Gao, M. Vissers, M. Sandberg, S. Chaudhuri, A. Sanders, L. Vale, K. Irwin, and D. Pappas, *J. Low. Temp. Phys.* **176**, 476–482 (2014).
- <sup>32</sup>K. O'Brien, C. Macklin, I. Siddiqi, and X. Zhang, *Phys. Rev. Lett.* **113**, 157001 (2014).
- <sup>33</sup>G. Dolan, *Appl. Phys. Lett.* **31**, 337 (1977).
- <sup>34</sup>A. D. O'Connell, M. Ansmann, R. C. Bialczak, M. Hofheinz, N. Katz, E. Lucero, C. McKenney, M. Neeley, H. Wang, E. M. Weig *et al.*, *Appl. Phys. Lett.* **92**, 112903 (2008).
- <sup>35</sup>R. Landauer, *IBM J. Res. Dev.* **4**, 391 (1960).
- <sup>36</sup>R. Bradley, *Nucl. Phys. B, Proc. Suppl.* **72**, 137 (1999).